Spatial Distribution of Surface Soil Moisture and Evaporation in a Small Watershed of Tiksi, Eastern Siberia

東シベリアティクシ近郊小流域に於ける表面土壌水分および蒸発の空間分布

Yinsheng ZHANG [1] Frontier Observational Research System for Global Change (FORSGC)
張　寅生 地球観測フロンティア研究システム
Tetsuo OHATA[1,2] Frontier Observation Research System for Global Change (FORSGC)/ Institute of Low Temperature Sciences, Hokkaido University
大畑哲夫 地球観測フロンティア研究システム/北海道大学低温科学研究所
Hiruyoki HIRASHIMA[2] Institute of Low Temperature Sciences, Hokkaido University
平島寛行 北海道大学低温科学研究所

To investigate the dependence of surface soil moisture and evaporation on topography, a 19-site network of observations was carried out in a small watershed near Tiksi, Eastern Siberia, during July 1999. A topographic index of relative elevation, the difference between the elevations of the observation sites and the stream (*DZ*), was the dominant factor affecting the spatial distribution of surface soil moisture and evaporation. Both surface soil volumetric water content and evaporation decreased as *DZ* increased, the former exponentially and the latter logarithmically. A significant difference was evident between adjacent regions to the east and west of the stream, even though *DZ* was the same.

Key word: Topography; soil moisture; evaporation

土壌水分および蒸発の地形依存性を調べるために、1999 年 7 月東シベリアティクシ近郊小流域において 19 点からなるネットワーク観測を行なった。比高(*DZ*)－観測点と近傍の流れとの高度差－が、表面の土壌水分および蒸発の空間分布に影響する支配的な要因である。*DZ* の増加につれて、表面の土壌水分、蒸発はともに減少する。しかし、前者は指数関数的に、後者は対数関数的に減少する。川を挟んで比較してみると、たとえ *DZ* が同じ値であっても表面の土壌水分および蒸発は東側と西側では違いが見られた。

キーワード: 地形; 土壌水分; 蒸発

Ⅰ. INTRODUCTION

Hydrological basins are usually characterized by obvious spatial variability, even when their area is small. The hydrological behavior of a watershed is influenced by many interacting factors, dominant amongst which is topography, which is an important factor in determining the hydrological response of a basin to climatic fluctuation, because it controls the movement of water within the basin. It also affects the

1 Frontier Observation Research System for Global Change (FORSGC), 3171-25, Showa-cho, Kanazawa-ku, Yokohama, Kanagawa, 236-0001 Japan
地球観測フロンティア研究システム, 〒236-0001 神奈川県横浜市金沢区昭和町 3171-25
2 The Institute of Low Temperature Science, Hokkaido University, Kita-19, Nishi-8, Kita-ku, Sapporo 060-0819, Japan
北海道大学低温科学研究所, 〒060-0819 札幌市北区北 19 条西 8 丁目

spatial distribution within the watershed of fluxes such as momentum, heat and moisture. Many articles discuss the effect of topography on various aspects of hydrological processes (*e.g.* Ander and Kneale, 1980; Beven and Wood, 1983; Boudreau and Rouse, 1995; Guo and Schuepp, 1994).

It has long been recognized that an improved approach to the spatial distribution of hydrological elements, like soil moisture and evaporation, would greatly aid modeling studies, particularly for distributed and physically based models using the contributing area concept. O'Loughlin (1986) proposed a predictive model of soil moisture distribution using a wetness index derived from a model requiring only a digital elevation model (DEM) and a value of transmissivity as inputs. Peschke et al (1990) discussed the spatial variability of hydrological processes in a small mountainous basin. Crave and Gascuel-odoux (1997) presented the influence of topography on the time and space distribution of soil surface moisture.

In the Arctic region, snow accumulation, redistribution of snow by wind, and snow ablation are important hydrological events each year. The continuous permafrost acts like an impermeable layer for ground water flow, confining subsurface flow to within the shallow active layer. Soil thermal and hydraulic properties change throughout the year because of thawing and freezing, or with changing moisture content. All of the hydrological components in the Arctic region are characterized by spatial variability.

Distribution of evaporation is determined by heterogeneity of soil moisture and atmospheric conditions. Within a fairly small watershed, the variability of atmospheric features would not be expected to be very significant; for such watersheds the surface soil moisture becomes a dominant factor affecting the spatial distribution of evaporation. In a cold region like the tundra area of Siberia, the dependence of evaporation on topography should be more apparent, because vegetation is predominantly sparse and low. Zhang *et al*. (1996) reported that differences in evaporation were observed at different positions along the profile of a hill in the Central Tibetan Plateau. In small-scale watersheds in permafrost regions, soil surface moisture often depends on location on the hillslope, owing to variation in the depth of the water table.

It is usual to employ networks of observation sites to investigate the spatial variability of soil moisture and evaporation, and construct a distribution function. For instance, the work of Crave and Gascuel-odoux (1997), which targeted the influence of topography on the spatial distribution of surface soil water content, was based on more than 400 soil samples across an area of 1.3 km^2. In the summer of 1999, a network of 19 observation sites was established in a small watershed near Tiksi, Siberia, to study the relation of surface soil water content and surface evaporation to topography.

Ⅱ. OBSERVATION

1. Location of observation region

The fieldwork for this study was supported by GAME/Siberia (GEWEX Asia Monsoon Experiment/Siberia). The observation site was located 7 km southeast of Tiksi, eastern Siberia ($71^0$35'N, $128^0$46'E, Figure 1), close to the Arctic Ocean. The Tundra Project of GAME/Siberia has conducted major observation programs covering heat budget, planetary boundary layer, surface and ground hydrology, isotopes, biology, and geocryology, since 1996. Several automatic weather stations, runoff gauges, grid networks for CALM (Circumpolar Active Layer Monitoring) and other networks have been established, and have continued in operation to the present.

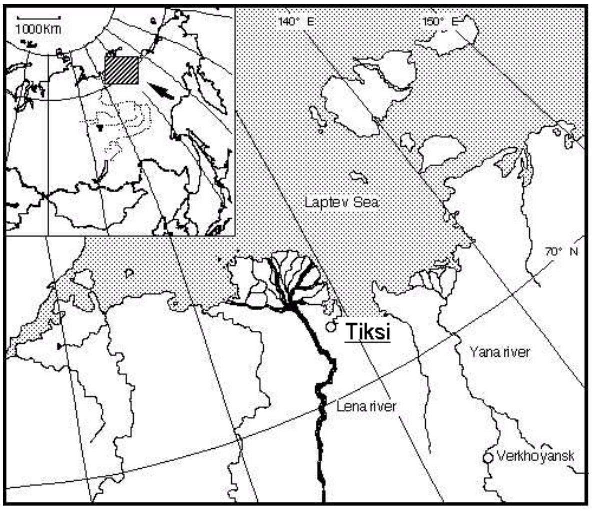

Figure 1. The location of Tiksi

2. Network of observations

Measurements were carried out from July 3 to July 26, 1999. Basically, the sites were set out along two lines (RR and AR in Figure. 2). The orientation of the main stream of the watershed ("T-river" in Figure 2) is east-west. The RR line ran perpendicularly across the T-river and to the AR line. Observation sites on the AR line, and sites 1-5 on the RR line, were set at intervals of 50 m, the others were spaced at 100 m. The RR line extending to the east of the T-river had an elevation range of about 40 m, with a mean slope of 200/1000, where the climate was drier and vegetation sparse. The part of the RR line to the west of the river had an elevation range of about 110 m, with a mean slope of 220/1000, with a relatively wetter climate and grass up to 30 cm high. At the top (west) end of the RR line (Site 11), a small area of snow pack persisted until July 20.

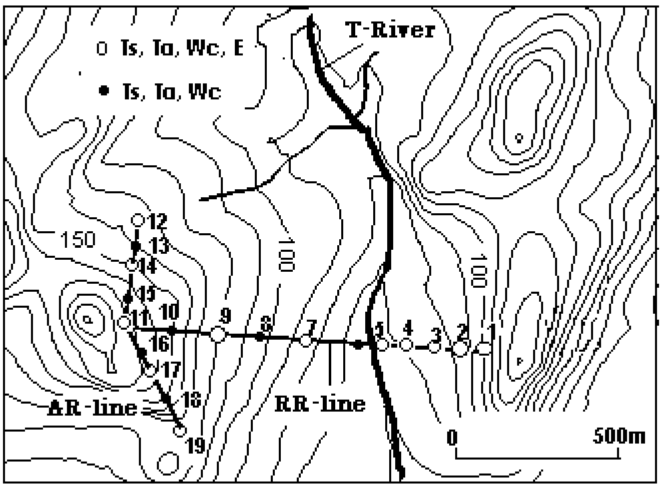

Figure 2. The observation network

Manual observations were recorded at noon each day, occasionally delayed by a few minutes, or even cancelled, when the weather was bad. As shown in Table 1, the elements observed included surface temperature, soil temperature in the surface layer, soil moisture in the surface layer and evaporation. Surface temperature was measured by radiation thermometers and soil temperature using conventional thermometers. Volumetric soil moisture in the surface layer was measured by time domain reflectometry

(TDR). Evaporation was measured by a micro-lysimeter method. The TDR and thermometer sensors, which extend over finite lengths, actually measured mean values over a depth of 10 cm.

Table 1. Elements observed over the network

Terms	Instrument	Depth (cm)	Number of observing points
Surface temperature (*Ts*)	Emission thermometer	Surface	19
Soil temperature (*Ta*)	Thermometer	0-10	19
Soil water content (*Wc*)	TDR	0-10	19
Evaporation (*E*)	Micro-lysimeter		12

The micro-lysimeter that we used to measure evaporation was a simplified version of the standard lysimeter, first developed by Boast and Robertson (1982). The device has attracted the interest of many other researchers (Shawcroft and Gardner, 1983; Martin *et al.*, 1994; Lascano and Van Bavel, 1986; Allen, 1990; Daamen, 1993), and has been used on the Tibetan Plateau (Zhang *et al.*, 1994) and in the Tianshan alpine region of China (Zhang and Zhang, 1999). As demonstrated by many researchers, with suitable design and careful operation, the micro-lysimeter method can provide reliable estimates of daily evaporation (Allen, 1990; Matthias et al, 1986; Daamen *et al.*, 1993; Shawcroft and Gardner, 1983). A cylindrical drum, 20 cm in diameter and 15 cm deep, was used here, set level with the surrounding soil surface and enclosing a mass of natural soil. Weight changes were measured every day, and thus the evaporation could be calculated from:

$$E=\Delta W/S+Pr \qquad (1)$$

where E is the evaporation, ΔW is the weight difference, S is the surface area, and, Pr is the precipitation. To permit adjustment for differences of temperature and moisture between the soil in the drum and in the surrounding soil, the temperature and moisture content of the soil in the drum were measured at the same time as observations in the surrounding soil.

3. Climate and ground condition in the observation area

The annual mean air temperature, relative humidity and wind speed are $-13.0\ ^0$C, 75% and 5.0 ms^{-1} respectively. The average annual precipitation is 345 mm. Precipitation in summer (from June to August) is normally 170 mm, showing a high year-to-year variability, ranging from 110 mm in 1987 to 290 mm in 1996 (Ishii *et al.*, 1998). In the period May to September 1998, the sensible heat flux measured ranged from –60 to 270 Wm^{-2}, and the latent heat flux ranged from –100 to 200 Wm^{-2}, calculated using 10-m tower profile observations. The Bowen ratio averaged 1.7 in the same period (Kodama *et al.*, 1998). Both of these studies were carried out at a location about 1 km south of the RR line. Snow covers the whole region from November to May, and a few small areas of snow pack persist until mid-July. The ratio of snow patch area was estimated to be 0.18 in June and 0.01 in August 1997 (Sato *et al.*, 1997).

The ground surface is covered by typical tundra plants, including mosses, lichens and sphagnum. The vegetation cover develops with spatial heterogeneity, with bare bedrock usually exposed at the summit of the hill. The leaf area index has been reported to vary from 3.42 to 3.59 using r = 0.1 m (side length of square, log m) and 0.87 to 1.21 at r = 0.01 m resolution (Sato *et al.*, 1999).

The soil in the area is thin and relatively undeveloped, consisting of poorly decomposed organic material overlying gravel or regolith. A multi-layered system has developed that consists of 0-0.2 m of accumulated organic material on 0.05-0.30 m of partially decomposed organic matter, over mineral silt above the permafrost (Watanabe *et al.*, 2000a). Table 2 lists the physical properties of the soil in the observation area, as measured in the summer of 1997 (Watanabe *et al.*, 2000b). The hydraulic conductivity of the organic soil was 10 to 100 times greater than that of the silt. The live-plant layer had a very high hydraulic conductivity as well. Thermal conductivity increased with depth.

Table 2. Characteristics of soil in observation area (after Watanabe *et al.*, 2000)

Type	Depth (cm)	Bulk density ($g\ cm^{-3}$)	Hydraulic conductivity ($cm\ s^{-1}*10^{-4}$)	Thermal conductivity ($Wm\ K^{-1}$)
Live-plant	0-5	0.21	$4.6\text{-}10^4$	0.23-0.74
Organic soil	0-19	0.25-1.01	4-140	0.70-1.21
Mineral silt	20-36	0.75-1.71	1.1-1.2	1.02-1.35

The region is typical of an area affected by continuous-permafrost, and the thawing table is thinner less than 1 m, even at mid-summer. Anisotropy and periodicity of the active layer thickness are produced by typical tundra polygon formation and soil fractionation. Mizoguchi *et al.* (1998) suggested that spatial variation in the thickness of the active layer is mainly due to vegetation cover, and the maximum thaw depth decreases with increasing thickness of the living plant layer (Watanabe *et al.*, 2000). The thawing depth has recently been reported to increase linearly with the “yellow level”, an index of vegetation cover defined by the mean value of yellow-colored pixels in digital GIS images (Ezaki *et al.*, 1999).

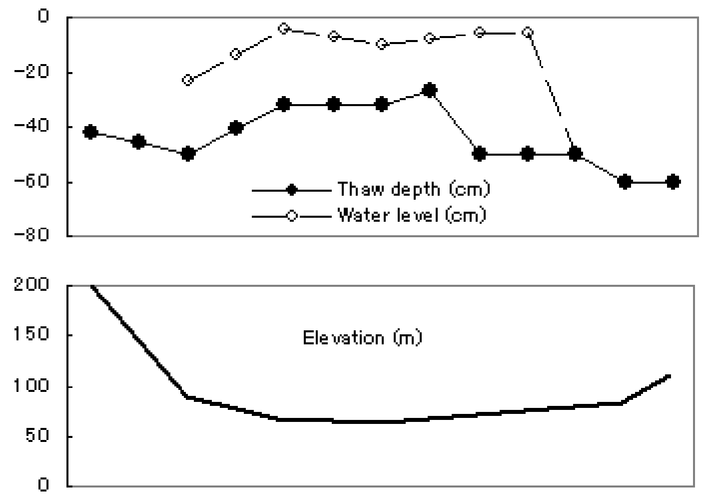

Figure 3. Profile of thaw depth and water level along the RR-line, the data are from Watanabe *et al.*, (2000), (the horizontal scale is different to following Figures).

The profile of thaw depth and water level along the RR line is shown in Figure 3; the data, from Watanabe *et al.*, (2000) were obtained during the summer of 1997. Briefly, the thawed layer becomes thinner as elevation decreases, and the thaw depth on the eastern side of the T-River is clearly greater than that on the western side. Bare bedrock is exposed at the high-level eastern end of the RR line. The profile of the water level along the RR line shows a similar difference. The water level is almost constant adjacent to the T-River, but becomes suddenly deeper approaching the summit at the eastern side, where the soil layer is too thin to retain water.

Ⅲ. RESULTS

Figure 4 shows the profiles of mean daily evaporation, soil moisture and soil temperature along the RR line (traversing the river), averaged over the observation period, for each site. Soil moisture and soil temperature averages shown are derived from the observations made each noon. Both evaporation and soil moisture decreased with increasing elevation. The soil at the hilltop was always drier, resulting in less evaporation. The soil temperature distribution did not show any defined pattern, but varied by about 6 ^{0}C.

The surface temperature covered a range of about 2 ^{0}C on the traverse across the river.

Averaging mean values across all sites on the RR line produced values of 18.0 ^{0}C for soil temperature at the surface, 4.7 ^{0}C within the surface layer, 35.1% for soil moisture content (volumetric) and evaporation of 2.1 mmday^{-1}. Comparing the data on different sides of the river, the eastern side showed lower evaporation (1.9 mmday^{-1}) than the western side, resulting from a lower soil moisture level (28.5%) and higher soil temperature (5.1 ^{0}C). The western side had a rather high mean moisture level (41.7%), producing a higher mean evaporation (2.2 mmday^{-1}), and lower mean soil temperature (4.4 ^{0}C).

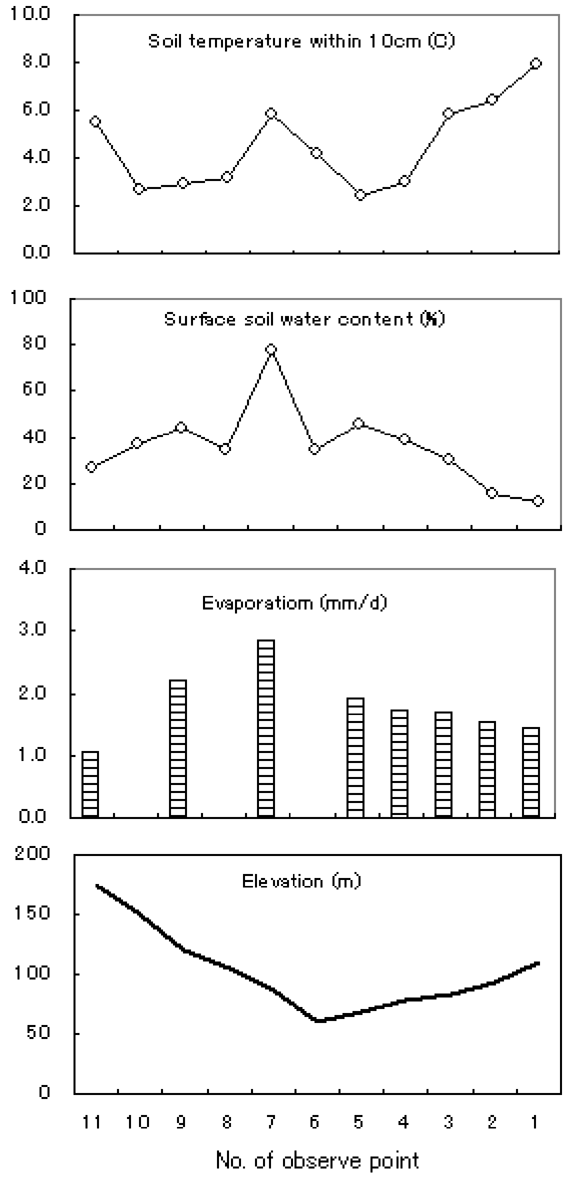

Figure 4. Averaged values along the RR-line

The results obtained at site 7 need to be discussed in more detail. Because of its atypical environment, the maximum values for all elements other than elevation were obtained there. The micro-topography was concave, and the grass grew to a height of 35 cm in July. Convergent flow produced frequent saturation in the surface soil layer. The mean moisture and evaporation were measured to be 78% and 2.9 mmday^{-1} respectively. Also, the lower albedo from the wet soil and well-developed grass must have resulted in greater radiation absorption, especially in the afternoon, thus explaining why the maximum soil temperature was observed there.

IV. ANALYSIS

1. Factors selecting

Determining the controlling factors is one of the more difficult aspects of spatial distribution analysis. There are two topographic factors often used in such studies at the present time: the Kirkby index, defined as the logarithm of the ratio between the cumulative upslope area and the tangent of the local slope, which determines the occurrence of soil saturation, and the index of elevation difference (*DZ*) between a given point and the stream, which refers more to the down-slope topography. Crave and Gascuel-odoux (1997) compared the significance of the Kirkby index and *DZ* to the spatial distribution of surface soil, and found that the water content of surface soil did not present a well-defined relationship with the Kirkby index, but did relate well to *DZ*. Therefore we have used *DZ* as the topographic index in this analysis, computed from a 10-meter scale digital elevation model (DEM).

As described above, this work was based on data from 19 sites over a period of 24 days. Variations in the data series derive from two sources, spatial and temporal variation. To eliminate the effects of temporal variation and derive a distribution function depending on spatial factors only, some transformation of the original data was necessary.

Considering the characteristics of the observed data as shown in Figure 3, the ratio of *Erat* and *Wrat* were defined as follows to elucidate the spatial distribution of evaporation and surface soil moisture:

$$Erat = E/E_s \quad \text{and} \quad Wrat = W_c/W_{cs} \qquad (2)$$

where E and W_c denote evaporation and soil moisture at any point respectively; E_s and W_{cs} are the evaporation and soil moisture at site 7, which was shown to be frequently in a saturated state. Since E_s and W_{cs} are constant for every set of observations, the series of *Erat* and *Wrat* contain only spatial variations.

2. Distribution of soil moisture and evaporation

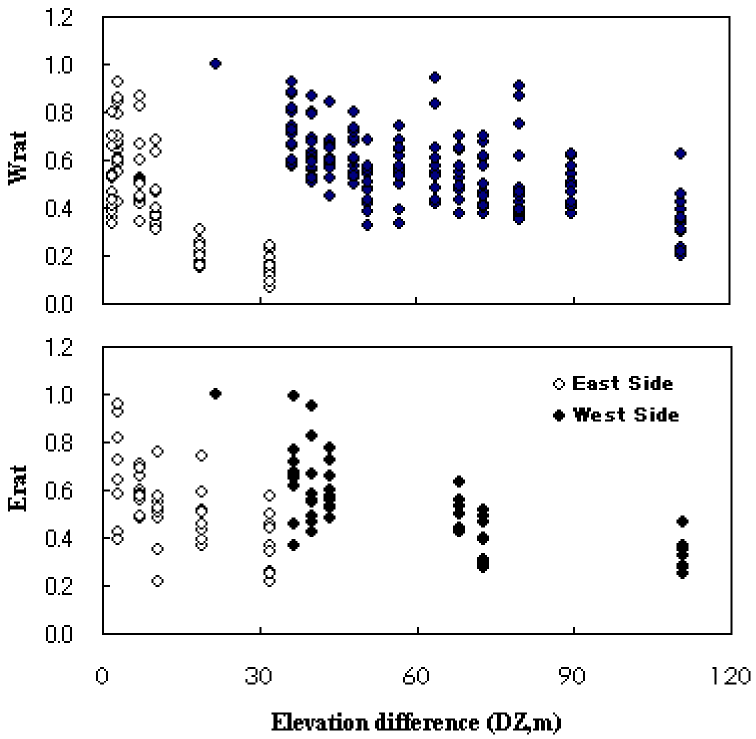

Figure 5. The variation of the *Wrat* versus *DZ* (up), and *Erat* versus *DZ* (down).

The variations of *Wrat* and *Erat* versus *DZ* are shown in the upper and lower panels of Figure 5 respectively. The *Wrat* values present two distinct distributions against the *DZ* topographic index. Both show the tendency of *Wrat* to decrease with increasing *DZ*. It is interesting that the data in the lower distribution were obtained on the eastern side of the river (at sites 1-5, Fig. 2), and the others are from the western side. The slopes of the east and west banks were similar, but the former was drier with poorer vegetation. It should also be pointed out that there was a small area of snow pack on the upper part of the western side, which one would expect to alter down-slope soil moisture content through the flux of melt water into the soil.

Similar distributions can be seen in the variation of *Erat* versus *DZ* (lower panel of Figure. 5). Both decreased with increasing *DZ* but at different rates. The spatial distribution of evaporation might have been related to other parameters, such as atmospheric conditions and vegetation, but at such a small spatial scale, the heterogeneity of vegetation would probably be related to the heterogeneity of soil moisture. Thus, the spatial distribution of evaporation was indeed determined by topography.

3. Simulating the spatial distributing pattern of soil moisture and evaporation

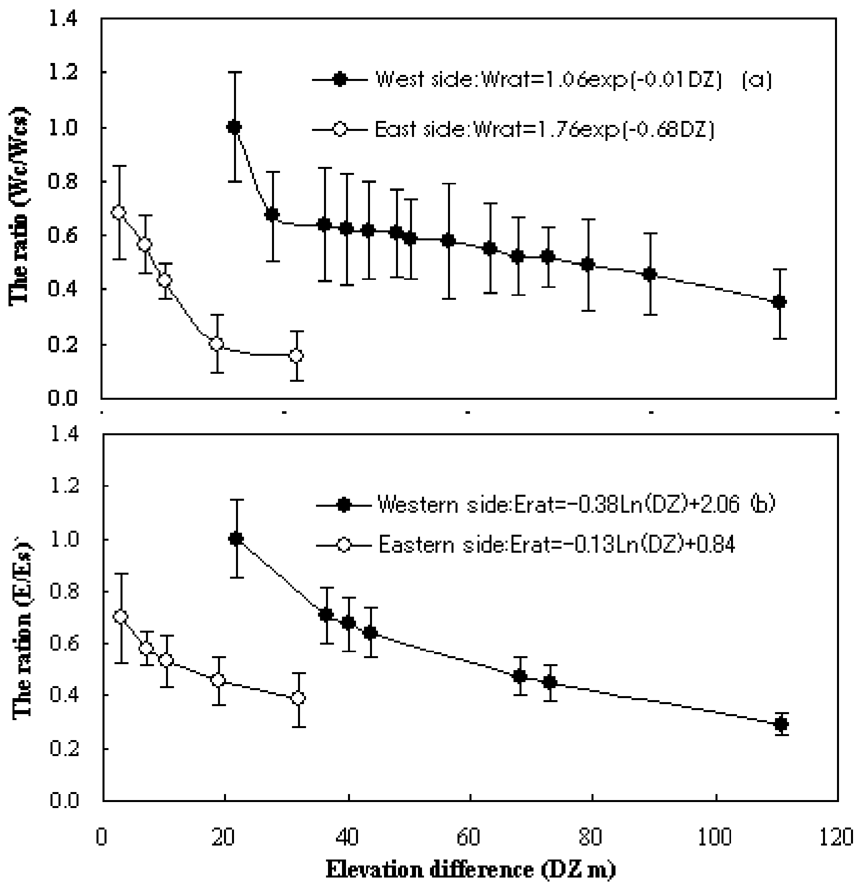

Figure 6. The simulation results of *Wrat* versus *DZ* (a) and *Erat* versus DZ (b).

From the data shown in Figure 5, a spatial distribution function of surface soil moisture within the study region can be derived, as shown in Figure 6 (a). After other trial analyses, an exponential function, defined as *Wrat*=*A*exp*BDZ,* was found to fit spatial variation of W/W_{cs} as a function of *DZ* for both the eastern and western sides of the river. Numerical values for A and B on the east and west banks of the T-river were obtained by regression analysis, and showed significant differences between the two sides.

There was a clear difference between the values of *Wrat* for the same value of *DZ* between the two sides of the river. Soil moisture seems more sensitive to topography at the lower part of the slope. On the western side of the river, the soil moisture decreases with *DZ* by 31% per 10 m when *DZ* is smaller than 30 m, but the rate is just 5.8% per 10 m when *DZ* is larger than 30 m. On the eastern side of the river, the rate is 19% per 10 m when *DZ* is smaller than 20 m, and just 3.8% per 10 m when *DZ* is larger than 20 m.

As shown in Figure 6 (b), the spatial distribution function of the ratio of *Erat* to *DZ* can be represented by a logarithmic function in the form $Erat = A_0 \ln DZ + B_0$. Evaporation decreases as *DZ* increases, as before. The coefficients A_0 and B_0 have different values for the two sides of the river. The difference in *Erat* between the two sides of the river for the same *DZ* value decreases as *DZ* increases. When *DZ* equals 20 m, the mean daily evaporation differs by 1.8 mmday^{-1} between the two sides of the river. When *DZ* equals 30 m, the difference becomes 1.2 mmday^{-1}. We present no data for the hilltop on the eastern side of the river, where bedrock was exposed.

4. Relationship of evaporation and soil moisture

The relationship of daily soil evaporation (*E*) to volumetric water content in surface layer with depths of 0 to 10 cm (W_c), showing in Figure 7, has been fitted with the regression equation:

$$E=1.06\ln(Wc)-1.61 \qquad (\mathrm{mmd}^{-1}) \qquad (3)$$

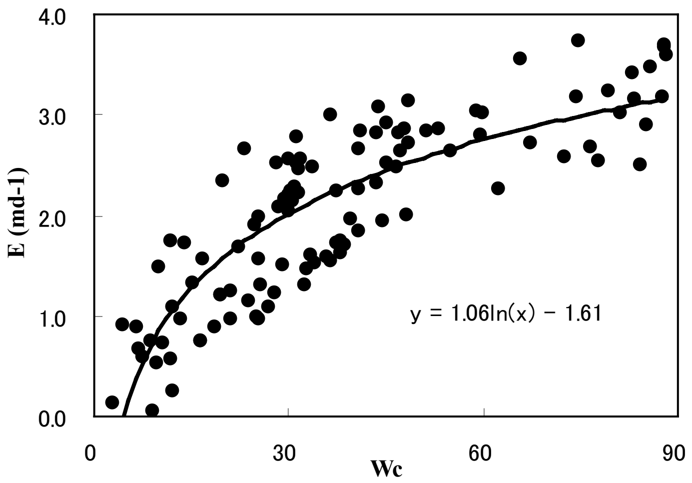

Figure 7. The relationship of daily evaporation (E) vs water content (Wc)

E varies logarithmically with *Wc*; this differs from some previous results (Shawcroft and Gardner, 1983; Zhang and Zhang, 1999; Zhang *et al.,* 1996) where *E* was found to increase exponentially with *Wc*. We anticipate that the results shown in Figure 7 will provide a valid technique to improve measurement of evaporation using micro-lysimeters. Shawcroft and Gardner (1983) found that results from a micro-lysimeter were less reliable when rain was falling. An improved way to use a micro-lysimeter in wet weather would be to establish a relationship between micro-lysimeter evaporation and the surface soil water content, and then use the surface water content measurement to infer evaporation.

V. SUMMARY AND DISCUSSION

Data from a network of observations clearly demonstrated spatial variability in the patterns of surface soil moisture and strongly correlated evaporation, despite the survey being over only a rather small area, with a maximum distance between sites of only 1 km. The difference in elevation of each site from the stream was an appropriate index to show the influence of topography on the spatial distribution of soil surface moisture and evaporation. Basically, the surface soil moisture decreased with the elevation difference between the site and the stream by an exponential function, and evaporation decreased by a logarithmic function. Similar spatial distribution patterns of surface soil moisture were found in a small catchment in France (Crave and Gascuel-odoux, 1997). The authors deduced an exponential spatial distribution function for surface soil moisture against *DZ/2*, which alters the regressive coefficients.

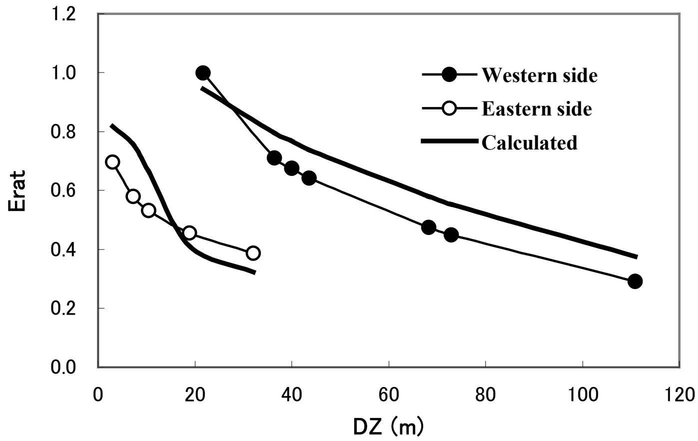

Fig. 8. Comparison of *Erat* shown in Fig.6 (b) and calculated by Eq. (3)

Within such a small region, the spatial variation of atmospheric conditions, which alters the potential evaporation, should be much lower. Therefore, it was only the soil moisture, and not other factors, that determined the spatial distribution pattern of evaporation in the study region. In other words, the redistribution of water on the ground surface, which is related to topography, controls the spatial distribution of evaporation. To support this deduction, evaporation was estimated from soil moisture over the network using Eq. (3), and compared with observations, as shown in Figure 8. The calculated curves agreed well with the results simulated from the observation data. The differences are believed to be explained by regression errors.

Surface soil moisture could definitely be related to other parameters, such as physical properties of the soil, vegetation and the thaw table. Significant differences in both surface soil moisture and evaporation were found between the western and eastern sides of the river, especially on the lower part of the slope. With increasing *DZ* the difference decreased. Thus, at the higher parts of a surface profile, surface soil moisture was expected to vary only with relative elevation, whereas significant differences were found at the lower parts of the catchment. Similar results were found by Crave and Gascuel-odoux (1997), and it was demonstrated that this was partly due to intrinsic factors, such as the soil's physical properties. This is clearly not consistent with the contributing source area concept, in which surface saturation is highly dependent on the time and space history of rainfall events. Similarly, the difference between the two sides of the T-river in the lower parts of the catchment might be clarified in terms of heterogeneity of vegetation. Unfortunately, the differences between the two sides of the stream were not investigated in detail. In summary, variability in both the physical properties of soil and vegetation should be taken into account in this type of investigation. This presents new challenges: for example, the spatial variability of the physical properties of soil and differences in transpiration for different types of plant will have to be defined.

Additionally, in such cold regions, the surface soil moisture and evaporation should correlate with the depth of snow that covers the ground for longer than 9 months. Firstly, deeper snow brings more melt water, which penetrates into the soil; secondly, deeper snow persists longer, thereby restraining evaporation and providing more run-on of water to the lower slope soils. It should be emphasized that the heterogeneity of atmospheric conditions such as precipitation, radiation and wind, played no part in this study. The applicability of the results, therefore, is limited to smaller spatial scales. The aim of this work was to reveal the effects of topography on water movement and, in turn, on evaporation, and it took no account of the spatial variation of precipitation and radiation processes. However, much has been reported on these processes, which could be employed to deal with hydrological heterogeneity at larger spatial scales. The benefits from this study are expected to be applicable to improving hydrological modeling and estimation of water budget components at the basin scale.

ACKNOWLEDGEMENT: The authors express their gratitude to the GAME/Siberia Project for supporting this field of study. They would also like to thank Dr. M. Kadota for his translation of abstracts of this paper. The authors are grateful to reviewers and the editor for their comments.

REFERENCE

Ander, M.G., and Kneale, P. E., (1980): Topography and hillslope soil wter relationships in a catchment of low relief, J. Hydrol., **47**, pp. 115-128.

Allen, S.J., (1990): Measurement and estimation of evaporation from soil sparse barley crops in northern Syria. Agric. For. Meteorol., **49**, pp. 291-309.

Beven, K.J., and Wood, E.F., (1983): Catchment geomorphology and the dynamics of runoff contributing areas, J. Hydrol., **65**, pp. 139-150.

Boast, C.W., and Robertson, T.M., (1982): A micro-lysimeter method for determining evaporation from bare soil: description and laboratory evaluation. Soil Sci. Soc. Am. J., **46**, pp. 689-696.

Boudreau, L.D., and Rouse, W.R., (1995): The role of individual terrain units in the water balance of wetland tundra, Climate Research, **5**, pp. 31-47.

Crave, A., and Gascuel-odoux, C. (1997) The influence of topography on time and space distribution of soil surface water content, Hydrol. processes, **11**, pp. 203-210.

Daamen, C.C., Simmonds, L.P., and Wallace, J.S., (1993): Use of micro-lysimeters to measure evaporation from sandy soils. Agric. Forest Meteorol., **65**, pp. 159-173.

Ezaki, T., Watanabe, K., Mizoguchi , M., and Kiyosawa, H., (1999): Estimating the spatial distribution of thaw depth in Siberia tundra near Tiksi from ground surface images relating with micro-undulation and vegetation, GAME Publ., **21**, pp. 23-24.

Guo,. Y., and Schuepp, P. H., (1994): On surface energy balance over the northern wetlands 1. The effects of small-scale temperature and wetness heterogeneity. J. Geophysucal Research, **99(D1)**, pp. 1601-1612.

Ishii, Y., Kodama, Y., Sato, N., Nakamura, R., and Nomura, M., (1998): Summertime water balance in a Siberia tundra basin, GAME Publ., **14**, pp. 13-16.

Kodama, Y., Sato, N., Yabuki, H., and Ishii, Y., (1998): Seasonal change in the heat fluxes over Siberia tundra, GAME Publ., **14**, pp. 27-34.

Lascano, R.J., and Van Bavel, C.H.M., (1986): Simulation and measurement of evaporation from a bare soil, Soil Sci. Soc. Am. J., **50**, pp. 1127-1132.

Martin, D.L., Wehner, D.L., and Throssell, C.S., (1994): Models for predicting the lower limit of the canopy-air temperature difference of two cool season grasses, Crop Sci., **34**, pp. 192-198.

Matthias, A.D., Salehi, R., and Warrick, A.W., (1986): Bare soil evaporation near a surface point-source emitter, Agric. Water Manage., **11,** pp. 257-277.

Mizoguchi , M., Watanabe, K., Fukumura, and K., Kiyosawa, H., (1998): Spatial distribution of active layer on a hillslope in Siberia tundra. GAME Publ., **14**, pp. 35-36.

O'Loughlin, E. M. (1986): Saturation regions in catchments and their relations to soil and topographic properties, J. Hydrol., **53**, pp. 229-246.

Peschke, G. *et al*., (1990): On the spatial variability of hydrologic processes in a small mountainous basin, *IAHS Publ*. No. **193**, pp. 61-69.

Sato, N.,, Kodama, Y., and Ishii, Y., (1997): Seasonal variation of water balance in Siberia tundra, GAME Publ., **10**, pp. 64-64.

Sato, T., Hayasaka, Y., Sakaguchi, H., Fukuhara, T., Yabuki, H., and Kodama, Y., (1999): Vegetation patterns and phyto-diversity in micro-scales on permafrost of Tiksi tundra, GAME Publ., **21**, pp. 25-32.

Shawcroft, R.W., and Gardner, H.R., (1983): Direct evaporation from soil under a row crop canopy, Agric. Meteorol., **28**, pp. 229-238.

Watanabe, K., Mizoguchi , M., Kiyosawa, H., and Kodama, Y., (2000a): Properties and horizons of active layer soil in tundra at Tiksi, Siberia, J. Japan Soc. Hydrol. & Water Resour., **13**, pp. 9-16.

Watanabe, K., Ezaki, T., Fukumura, K., Mizoguchi , M., and Kiyosawa, Y., (2000b): Variability of thaw depth depending on surface micro-undulation and vegetation cover in the Siberian Tundra, GAME Publication, **31(3**), pp. 632-636.

Zhang, W., and Zhang, Y., (1999): Observation and estimation of daily actual evapotranspiration and evaporation on a glacierized watershed at the headwater of the Urumuqi River, Tianshan, China, Hydrol. Processes, **13**, pp. 1589-1601.

Zhang, Y., Pu, J., and Yao, T., (1994): The climatic feature at the Tanggula Mountain Pass on the center of Qingzang Plateau. Journal of Glaciology and Geocryology, (In Chinese with English abstract), **16(1)**, pp. 41-48.

Zhang, Y. Pu, J., and Yao, T., (1996): Evaporation from ground surface observed in the Tanggula Pass in the center of Tibet Plateau, Cryosphere, **2**, pp. 50-54.